Phase effect on flow control for dielectric barrier plasma actuators

K. P. Singh and Subrata Roy[a)]
Computational Plasma Dynamics Laboratory, Mechanical Engineering, Kettering University, Flint, Michigan 48504

(Received 3 March 2006; accepted 16 May 2006; published online 6 July 2006)

Active control of flow has a wide range of applications. Specifically, mitigation of detachment due to the weakly ionized gas flow past a flat plate at an angle of attack is studied using two asymmetric sets of electrode pairs kept at a phase lag. The equations governing the dynamics of electrons, helium ions, and neutrals are solved self-consistently with charge-Poisson equation. The eletrodynamic forces produced by two actuators largely depend on the relative phase between the potentials applied to rf electrodes and distance between them. A suitable phase and an optimum distance exist between two actuators for effective separation control. © *2006 American Institute of Physics*. [DOI: 10.1063/1.2218770]

Plasma-based actuators are advantageous for their absence of moving parts, rapid on-off deployment, and attractive self-limiting characteristics. In recent years, experimental observations have shown the capability of dielectric barrier devices, operating at relatively low power (a few watts) levels, in a wide range of applications to suppress separation. Wings and fuselage of aircraft may be covered with a thin layer of glow discharge plasma which can provide, through Lorentzian collisions, a purely electrohydrodynamic coupling between an electric field and the neutral gas in the boundary layer which is helpful in reattachment of flow.[1]

An asymmetric single dielectric barrier plasma actuator consists of two electrodes separated by a dielectric. The upper electrode is exposed to the free stream flow, while the lower electrode is placed slightly downstream underneath the dielectric. The two electrodes may overlap horizontally with each other. A voltage fluctuating at rf is applied to the electrodes exposed to the gas. It has been suggested that the thrust produced by the actuator depends not only on the shape and position of the exposed electrode;[2,3] it may also be enhanced using a polyphase power supply to the electrodes.[1]

The plasma when energized emits an acoustic signal which can provide information about generated electric force.[4] Different electrode configurations have also been developed[1,5] and numerically experimented with[6–8] for determining the dependence of the ionization on input voltage, frequency, and electrode geometry. Accurate optimization of actuator performance will depend on further understanding of the role of peristaltic mechanism conjectured in Ref. 1.

The present authors have carried out simulation study of an asymmetric single dielectric barrier plasma actuator.[3,4,6–8] They have shown that net force on the charge separation is in the positive-x direction and negative-y directions. In this letter, we study the effect of relative phase and the streamwise gap d between the actuators on the interaction between the plasma and surrounding gas using two sets of dielectric barrier plasma actuators located at a distance. We solve the equations governing dynamics of electrons, ions, and fluid to obtain spatio-temporal profiles of electron density, ion density, electric potential, fluid density, and fluid velocity.

Figure 1 describes the schematic for the present computational study. The simulated region is 15 cm long and 5 cm high. The lower part of the domain consists of a 0.1 cm thick insulator with dielectric constant $\varepsilon_d=3.5\ \varepsilon_0$ while the upper part is filled with inert helium gas of $\varepsilon_f=1.0055\varepsilon_0$, where ε_0 is the permittivity of the free space. The rf and grounded electrodes are 1.2 and 1.27 cm in length, respectively. The rf and grounded electrodes are taken at $y=0.1$ cm and $y=0$ cm with 0.02 cm overlap along the x axis. The overlap between the first pair of electrodes is from $x=1.5$ to 1.52 cm, and the position of overlap between the second pair of electrodes is varied to see the effect. The thickness of the electrodes is infinitesimally small. The embedded electrode is grounded; a sinusoidal voltage $\phi=\phi_0 \sin(2\pi ft)$ is applied to the first actuator, and $\phi=\phi_0 \sin(2\pi ft+\theta)$ (where θ is the relative phase between two rf potentials) is applied to the second actuator. The frequency and potential of excitation are fixed at $f=5$ kHz and $\phi_0=300$ V, respectively. The gas is preionized with initial plasma density $n_0=5\times10^{10}$. The initial velocity components u_0 (along the x direction) and v_0 (along the y direction) are 1000 and 200 cm/s, respectively, corresponding to an angle of attack (α) of approximately 12°. The separated region observed in the vicinity of the dielectric surface is then subjected to control with suitably located two dielectric barrier plasma actuators.

The drift-diffusion form of continuity and Poisson's equations for the electrons and ions are solved together with the fluid momentum and continuity equations as described in Refs. 3, 6, and 9. The self-consistent formulation is solved using a Galerkin variational formulation based finite-element method[8] to obtain electron, ion, and neutral velocities and densities, and electric potential. The no-slip condition is as-

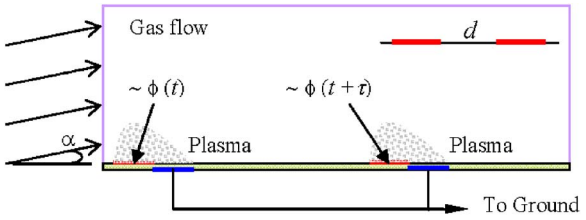

FIG. 1. (Color online) Schematic of two asymmetric single dielectric barrier plasma actuators with an incident neutral gas flow angle α.

[a)]Author to whom correspondence should be addressed; electronic mail: sroy@kettering.edu

 © 2006 American Institute of Physics
Downloaded 06 Jul 2006 to 158.80.0.225. Redistribution subject to AIP license or copyright, see http://apl.aip.org/apl/copyright.jsp

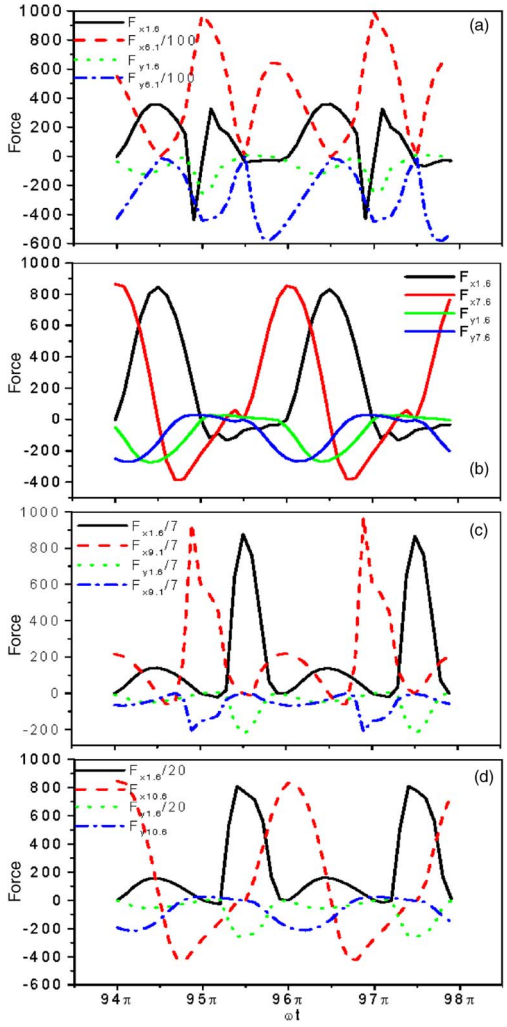

FIG. 2. (Color online) The force components per unit volume (dyne/cm^3) as a function of ωt at (a) $x=1.6$ cm and $x=6.1$ cm, (b) $x=1.6$ cm and $x=7.6$ cm, (c) $x=1.6$ cm and $x=9.1$ cm, and (d) $x=1.6$ cm and $x=10.6$ cm.

sumed for the gas neutrals at the dielectric surface, and the velocity at the left boundary of the upper domain is set to the free stream condition at all times. Homogeneous Neumann conditions are applied to the upper edge of the domain. For the charge equations, the total current continuity is ensured across the dielectric interface, i.e., at this location, conduction, convection, and displacement currents in the gas are balanced with the displacement current in the dielectric. A small secondary emission current is also considered at dielectric and electrode surfaces.

We have run a few cases to see the effect of phase difference between rf voltages applied to two actuators. We have determined (all cases not shown for brevity) that relative phase difference $\theta=\pi/2$ between two rf voltages gives the best effect for separation control. The results reported in this letter are for this value of phase difference. As mentioned earlier, the overlap between the first pair of electrodes is from $x=1.5$ to 1.52 cm. Four cases with streamwise interelectrode distances $d=4.5$, 6, 7.5, and 9 cm are studied in parts (a), (b), (c), and (d), respectively, of each of the figures described below. For these cases, the position of overlap between the second set of electrodes is from $x=6$ to $x=6.02$ cm, $x=7.5$ cm to $x=7.52$ cm, $x=9$ cm to $x=9.02$ cm, and $x=10.5$ cm to $x=10.52$ cm, respectively. A comparison between the figures shows the effect of relative distance between actuators.

Figures 2(a)–2(d) show force components F_x and F_y per unit volume as a function of ωt for the cases studied. The force is large near the dielectric surface and near the overlap between two electrodes of an actuator. Hence, the time varying force results are described at selected points at $y=0.2$ cm and near the overlap between two electrodes of an actuator. The first point of observation is at $x=1.6$ cm for each figure, and the second point is at $x=6.1$, 7.6, 9.1, and 10.6 cm for Figs. 2(a)–2(d), respectively. It can be seen that for $d=4.5$ cm the magnitude of both the components of force is two orders of magnitude higher at $x=6.1$ cm than at $x=1.6$ cm in Fig. 2(a). The magnitude of force at $x=7.6$ cm is

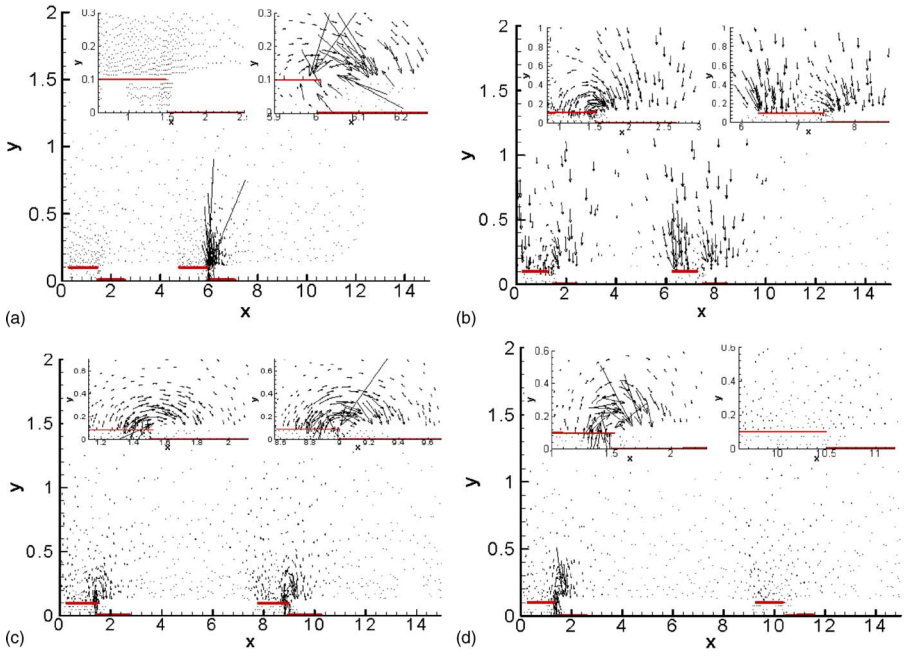

FIG. 3. (Color online) Time-averaged force distribution. The actuators are (a) 4.5 cm, (b) 6 cm, (c) 7.5 cm, and (d) 9 cm apart; x and y are in centimeters.

Downloaded 06 Jul 2006 to 158.80.0.225. Redistribution subject to AIP license or copyright, see http://apl.aip.org/apl/copyright.jsp

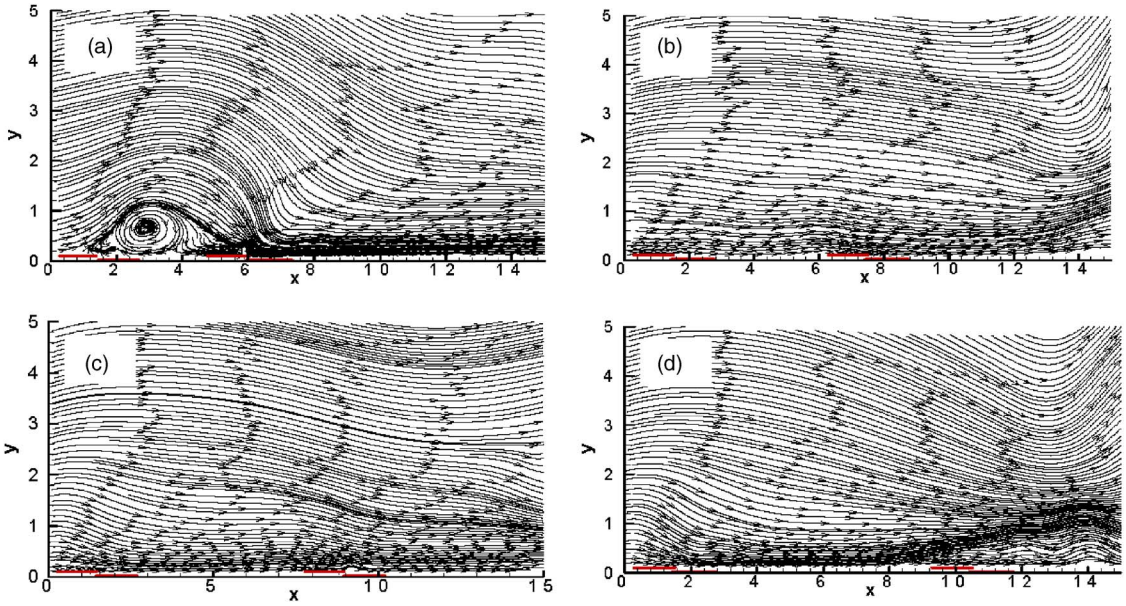

FIG. 4. (Color online) The gas velocity vectors and streamlines. The actuators are (a) 4.5 cm, (b) 6 cm, (c) 7.5 cm, and (d) 9 cm apart.

nearly equal to that at $x=1.6$ cm for $d=6$ cm. Temporal variation of force components is not similar in Figs. 2(a) and 2(b). Magnitude and temporal variation of the force components at $x=9.1$ cm are nearly equal to the force components at $x=1.6$ cm in Fig. 2(c) for $d=7.5$ cm. Figure 2(d) shows that for $d=9$ cm, the force magnitudes at $x=10.6$ cm are nearly 20 times lower than that at $x=1.6$ cm. Temporal variation of the force at $x=1.6$ cm also does not follow the force at $x=10.6$ cm. Figures 3(a)–3(d) show vectors of time-averaged force distribution for the cases studied. The insets in each figure show the zoomed in view and highlight the relative magnitude and direction of force distribution about exposed electrodes. Clearly, Fig. 3(c) has the best forward moving force distribution amongst these cases, and the streamwise force vectors about the downstream electrode are nearly twice as large as that in the upstream.

Figures 4(a)–4(d) show gas velocity vectors and streamlines of velocity for the reported cases. A new separation bubble is created downstream of the first actuator in Fig. 4(a). The neutrals have a high velocity in the x direction near the dielectric surface from $x=7.5$ cm to $x=15$ cm. The velocity vectors point towards the positive-y direction from $x=13$ cm to $x=15$ cm, and separation is not eliminated fully in Fig. 4(b). The velocity vectors point towards the positive-x direction throughout close to the dielectric surface, and separation is eliminated (but for a tiny bump near $x=9$ cm) in Fig. 4(c). The velocity vectors are tilted towards the positive-y direction from $x=8$ cm to $x=15$ cm, and separation is not eliminated in Fig. 4(d).

The following inferences can be made from the above figures. The temporal evolution of the forces will follow each other if two actuators are located in a noninteractive range. If both actuators work in equilibrium with each other, the force produced by one nearly balances the other. When the actuators are at an interactive distance, spatial and temporal density profiles are affected by each other, which in turn affect charge separation and force produced by the actuators. For cases (a) and (d) in the above description the forces produced by actuators are not balanced by each other, which results in either formation of new separation bubble or imperfect separation control. The induced forces by actuators are nearly balanced between the two actuators in cases (b) and (c). The location of the second actuator is closer to the right edge of the domain in (c) than in (b). Thus, the separation is controlled over the full domain in Fig. 4(c), but it is not controlled from $x=13$ cm to $x=15$ cm in Fig. 4(b). The most favorable situation for separation control is when forces exerted by actuators are balanced by each other while the induced forces about the downstream electrode are slightly larger. In conclusion, the interaction between the forces can be optimized and the separation is eliminated most effectively for a certain phase difference between the actuators and distance between them.

This work is partially supported by the Air Force Research Laboratory contract and grant support from the AFOSR, with Dr. John Schmisseur and Lt. Col. Rhett Jefferies as technical monitors.

[1] J. R. Roth, Phys. Plasmas **10**, 2117 (2003).
[2] C. L. Enloe, T. E. McLaughlin, R. D. Van Dyken, K. D. Kachner, E. J. Jumper, T. C. Corke, M. Post, and O. Haddad, AIAA J. **42**, 595 (2004).
[3] S. Roy, Appl. Phys. Lett. **86**, 101502 (2005).
[4] D. V. Gaitonde, M. R. Visbal, and S. Roy, 44th Aerospace Sciences Meeting, Reno, Nevada, 10 January 2006, Paper AIAA-2006-1205.
[5] T. C. Corke and M. L. Post, 43rd Aerospace Sciences Meeting, Reno, Nevada, 10 January 2005, Paper AIAA-2005-0563.
[6] K. P. Singh and S. Roy, J. Appl. Phys. **98**, 083303 (2005).
[7] S. Roy and D. V. Gaitonde, Phys. Plasmas **13**, 023503 (2006).
[8] S. Roy, K. P. Singh, and D. Gaitonde, Appl. Phys. Lett. **88**, 121501 (2006).
[9] E. E. Ferguson, F. C. Fehsenfeld, and A. L. Schmeltekopf, Phys. Rev. **138**, A381 (1965).

Downloaded 06 Jul 2006 to 158.80.0.225. Redistribution subject to AIP license or copyright, see http://apl.aip.org/apl/copyright.jsp